Review of Scientific Instruments | ARTICLE | pubs.aip.org/aip/rsi

Advanced electron beam lithography strategies for fabrication of high-precision VLS x-ray gratings

Cite as: Rev. Sci. Instrum. 96, 121302 (2025); doi: 10.1063/5.0299358
Submitted: 27 August 2025 • Accepted: 31 October 2025 •
Published Online: 1 December 2025

Kevin Hofhuis,[1,a)] Nazanin Samadi,[1] Bjarke A. Frederiksen,[1] Konstantins Jefimovs,[1] Analía F. Herrero,[2,3] Tino Seliger,[2] Frank Siewert,[2] Bas Ketelaars,[4] Christiaan Zonnevylle,[4] Vitaliy A. Guzenko,[1] and Christian David[1]

AFFILIATIONS

[1] PSI Center for Photon Science, Paul Scherrer Institute, 5232 Villigen PSI, Switzerland
[2] Helmholtz-Zentrum Berlin für Materialien und Energie, Albert-Einstein-Str. 15, 12489 Berlin, Germany
[3] Physikalisch-Technische Bundesanstalt, Abbestr. 2-12., 10587 Berlin, Germany
[4] Raith B.V., De Dintel 27, 5684 PS Best, The Netherlands

Note: This paper is part of the Special Topic on The 8th International Workshop on X-Ray Optics and Metrology.
[a)]**Author to whom correspondence should be addressed:** kevin.hofhuis@psi.ch

ABSTRACT

We present advanced electron beam lithography (EBL) strategies for the fabrication of high-precision variable-line-spacing (VLS) x-ray gratings with sub-nanometer pitch control on large, curved silicon substrates up to $140 \times 30 \times 10$ mm^3. Our approach employs a novel non-linear dose mapping methodology, combining dynamic field scaling and multi-pass writing techniques with HSQ resist to enable precise control over pitch. The resulting grayscale lithography resist patterns are transformed into blazed grating profiles via through-mask oxidation, which leverages different silicon oxidation rates for accurate topography transfer. The implementation of newly developed dose gradient shapes dramatically improves data handling efficiency and promotes stable, reliable exposures. We validate our methods experimentally through laser goniometer measurements, which confirm a third order polynomial line density agreement between designed and fabricated pitches across the optical area of 120×20 mm^2. Unlike mechanical ruling, where throughput decreases with increasing line density, our EBL approach maintains constant throughput regardless of the grating line density, providing unique flexibility not limited to single lines but also allows for complex freeform x-ray optics in the future. This work thus demonstrates the scalable fabrication of high-quality x-ray VLS gratings, advancing the prospects for next-generation optical components at synchrotrons and free-electron lasers.

INTRODUCTION

Variable line spacing (VLS) gratings[1] with continuously varying line densities represent critical components for advanced applications of soft x rays at synchrotron and free-electron laser facilities, where spectral resolution requirements demand nanoscale line placement accuracy.[2–4] These blazed diffraction gratings achieve diffraction efficiencies that are substantially higher than that of their counterparts with laminar line profiles. In particular designed for certain wavelengths and diffraction orders [see Fig. 1(a)], it makes them essential for monochromators, resonant inelastic x-ray scattering analyzers, self-seeding schemes, and pulse compression systems.[5–8] Furthermore, they are essential for experiments at free electron lasers as their damage threshold is higher than for lamellar gratings.[9,10] Currently, blazed x-ray gratings are mainly produced by mechanical ruling techniques, with only one mechanical ruling facility available in Europe[11] and very few further in Japan and the US. In addition to the resulting supply shortage and long lead times for the production of ruled gratings, the method also has several technological limitations: (i) for large gratings and high line densities, the duration of the ruling process becomes very long and thus expensive, (ii) the method is limited regarding the production of gratings with shallow blaze angles, and (iii) the method is fundamentally limited regarding possibility to produce several different gratings on the same substrate or to produce gratings with curved lines.

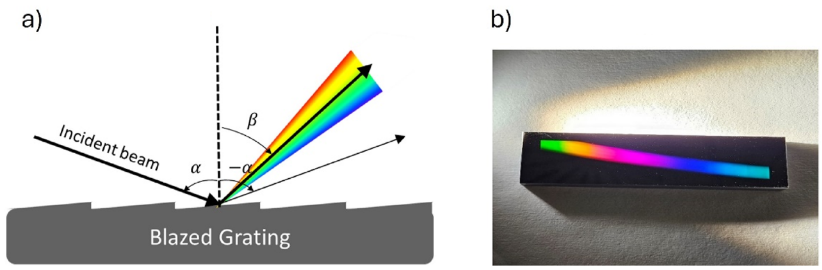

FIG. 1. Blazed grating design and curved-substrate implementation. (a) Schematics of the blazed grating profile displaying incident beam angle α, blaze angle β, and diffracted orders for optimized groove geometry. (b) Photograph of a variable-line-spacing (VLS) grating patterned onto a curved silicon substrate, demonstrating uniform groove formation over the 120 mm length.

We demonstrate that advanced electron beam lithography (EBL) strategies combining grayscale exposures, continuous field scaling,[12] multi-pass exposures, and novel non-linear dose exposure techniques achieve sub-nanometer pitch control across the entire large curved silicon substrates up to 140 × 30 × 10 mm^3. In this, we use high-energetic electrons to alter a flowable oxide known as the resist to generate a height-varying structure that is then transferred into the silicon substrate. An example of such a fabricated VLS grating on a curved silicon substrate demonstrating uniform groove formation across its full length is given in Fig. 1(b). Our approach of using e-beam lithography seeks to address the critical bottleneck in manufacturing high-precision optical components, while enabling fabrication on curved substrates. Critically, it also enables scaling to higher line densities without time penalties, which is a key advantage over mechanical ruling.

Technical requirements and fabrication challenges

The fabrication of VLS gratings on curved silicon substrates presents unique geometric challenges, particularly with structure height variations reaching 10–20 nm (resist 100–200 nm) across the writing area, making it important to do appropriate field correction strategies for tilt and curvature and choose a fitting contrast curve (Fig. 3). Since we require slowly varying grooves that are in the 1250 nm pitch range, we decided to use a short development time allowing for precise height variations according to delivered doses. Furthermore, the VLS patterns require continuously varying line densities (varying pitch) following polynomial relationships of the form $a_0 + a_1x + a_2x^2 + a_3x^3$,[3,13] (see Table I for parameters), and the polynomial is dependent on various parameters based on the beamline and application. These VLS parameters are key to ensure optical performance, groove-profile fidelity, and correct (anti-)blaze angles.[5] To fulfill all requirements for such a grating, the quality of the Si-substrate has to be excellent. Including slope error <1 μrad rms and a micro-roughness below 0.3 nm rms. Finally, the precise knowledge of the radius of curvature is essential to define the polynomial for the required VLS-parameter. In our case, the substrate characterization was performed at the BESSY optics laboratory using slope measuring deflectometry[14] and with light interferometry.[15]

We address these challenges through employing our Raith EBPG5000 Plus e-beam writer system equipped with a universal pattern generator, enabling newly developed dose gradient shapes to be exposed together with multi-pass and combined with field scaling to achieve sub-nanometer average pitch placement accuracy. The field scaling technique dynamically stretches or compresses the 1 mm mainfield (incl. the subfields inside) by up to ±1%, allowing precise control over the line placement that surpasses the addressing grid limitations of the deflection system. Further technical details on the field scaling function can be found in the Raith EBPG system manuals and are also exemplified in previous scientific work.[12] For VLS gratings with continuously varying line densities, we assume one mainfield to be at a single line density. For writing, we employed specific EBL parameters: a 100 kV acceleration voltage, beam currents of 150 nA, dose values between 250 and 5000 $\mu C/cm^2$ for the Hydrogen silsesquioxane (HSQ) resist, write field sizes of 80 × 860 μm^2 (larger size along the lines), and a beam-step size of 25 nm. The total writing time is slightly less than 100 hours for the entire grating of 120 × 20 mm^2.

TABLE I. Comparison of specified and measured polynomial coefficients for VLS grating.

Parameter	Specified	Measured	Residuals
Gratings density (a_0)	800 l/mm	800.001 l/mm	0.001 l/mm
First coefficient (a_1)	2.81 mm^{-1}	2.8082 mm^{-1}	0.002 mm^{-1}
Second coefficient (a_2)	2.2×10^{-3} mm^{-2}	2.195 mm^{-2}	5×10^{-6} mm^{-2}
Third coefficient (a_3)	6.4×10^{-6} mm^{-3}	6.6×10^{-6} mm^{-3}	2×10^{-7} mm^{-3}

Non-linear dose mapping implementation

Electron beam lithography (EBL) is a technique that uses focused beam of electrons to create extremely precise patterns on a surface coated with a sensitive material called resist. By carefully controlling the electron dose, grayscale EBL produces smooth, three-dimensional structures with nanoscale height variations, which are essential for manufacturing high-performance x-ray optical components, such as blazed VLS gratings.

We developed a breakthrough advancement in grayscale lithography data preparation through non-linear dose mapping that enables precise exposure control at the beam step size level (see Fig. 2), in particular applicable for the Raith EBPG plus tools with a universal pattern generator as a software update, released per early 2025. This method represents a shift from conventional fracturing approaches, where each dose assignment traditionally required separate geometric shapes, leading to exponential increase in the data file sizes and processing complexity. Integrated dose modulation is supported in basic shapes, such as rotated rectangles, circles, and circle parts [see Fig. 2(c)].

A major advantage is the implementation of the dose mapping feature, which is between normalized positions. This can be used to implement your process curve, contrast curve, and many other information. The normalized positions allow the full, or partial, use of the dose map on any desired shape size and resolution settings. In particular, because the dose gradient shapes can be picked from where it starts on the dose mapping and where it ends. The example in Fig. 2(b) considers the use of the full range, but the method is not limited to this. Then, based on the size of the basic shape and the beam-step-size, the amount of dose changes becomes fixed. Even if the dose mapping contains a limited number of points, the system interpolates the remaining values.

The impact of this methodology becomes evident when considering large-area VLS grating fabrication. A comparative analysis of a 120 × 20 mm^2 VLS grating design demonstrates improvement in data handling efficiency. Conventional fracturing methods generated a 146 GB ASCII file containing 38 × 10^9 individual shapes, while our dose mapping approach reduces this to 30 MB ASCII files with only 950 × 10^6 shapes, representing a nearly 5000× reduction in the file size while maintaining identical pattern fidelity. This efficiency gain facilitates faster pattern processing, simplified debugging procedures, and enhanced reliability during extended exposure sessions.

Through-mask oxidation process integration

We seamlessly integrate the developed dose gradient shapes methodology with a novel through-mask oxidation technique for pattern transfer to silicon substrates.[16] Using a negative hydrogen silsesquioxane (HSQ) resist as a grayscale mask, precisely controlled dose variations create corresponding thickness modulations that translate to differential oxidation rates during subsequent dry thermal processing. This approach enables fabrication of blazed grating structures with smooth surface finishes while maintaining sub-nanometer placement accuracy achieved during the lithographic step.

The fabrication process, see Fig. 3, begins with grayscale lithography using HSQ resist as both the exposure medium and precursor material for subsequent through-mask oxidation. HSQ is spin-coated to ~300 nm thickness on the (thick curved) silicon substrates, followed by dose-modulated exposure. During grayscale exposure, the HSQ resist undergoes localized cross-linking in direct proportion to the electron dose delivered. This process converts the exposed regions of HSQ into silicon oxide, forming a grayscale mask whose thickness profile accurately reflects the spatially varying electron dose pattern. After development and oxide removal, the resulting mask exhibits thickness variations that correspond directly to the intended blazed grating profile. This enables precise pattern transfer to the silicon substrate in the subsequent through-mask oxidation step, as described in Ref. 17. The through-mask oxidation technique leverages differential oxidation rates of silicon substrate areas protected by a layer of HSQ with varying thicknesses under dry oxidation conditions at 1100 °C (see Fig. 3 for the process depiction). Thinner HSQ regions allow faster silicon consumption during oxide growth; the thicker ones slow down this process. This procedure effectively transfers the grayscale resist profile into the underlying silicon substrate, creating the desired blazed grating geometry.

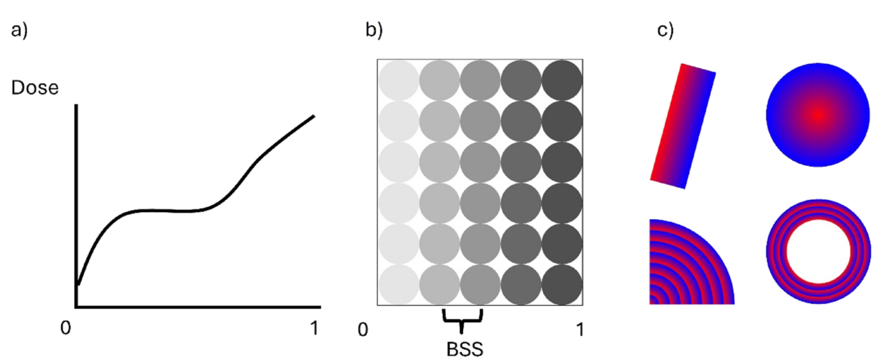

FIG. 2. Non-linear dose mapping implementation enables direct dose variation embedding within geometric primitives for enhanced lithographic efficiency. (a) Dose mapping function demonstrating non-linear relationship between normalized position (0–1) and dose variations for precise pattern control. (b) Dose gradient cube methodology illustrating systematic dose distribution across a 5 × 6 array grid with grayscale values directly embedded in the BSS (beam step size) framework. (c) Basic geometric shapes, including rectangles, circles, sectors, and rings, demonstrating fundamental primitives that support integrated dose modulation.

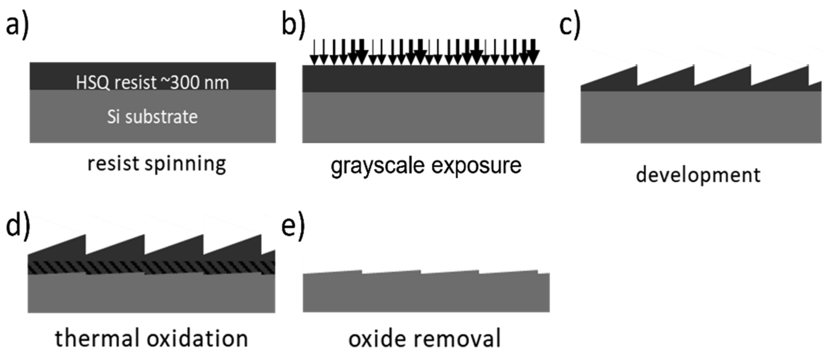

FIG. 3. Through-mask oxidation for smooth surfaces. Step-by-step process for the through-mask oxidation process. (a) HSQ spincoated on the Si substrate, then (b) grayscale exposure using the dose gradient shapes, and (c) subsequent development in AZ 351B diluted with water 1:3. (d) Thermal oxidation based on the desired final grating heights and (e) oxide removal in HF.

RESULTS AND VALIDATION

The through-mask oxidation method is practically limited to a maximum of 100 nm Si height differences, which was achieved using 700 nm HSQ [Fig. 4(a)–contrast curve] and longer oxidation, see Fig. 4(b) for the 480 nm oxidation at 90 s development time. However, this creates quite shallow anti-blaze angles due to the process blur. Hence, for our gratings, an intermediate value of 300 nm HSQ and 55 nm oxidation was used, resulting in 20 nm height variations.

AFM imaging shows a characteristic sawtooth roughness on the substrate [Fig. 5(a)], while after oxidation and oxide removal, the sawtooth profile is transferred into silicon [Fig. 5(b)]. This surface quality enhancement represents a critical advantage of this approach, achieving a tenfold reduction in height variations as demonstrated by AFM measurements comparing surface roughness before and after oxidation.[18] Final oxide removal using hydrofluoric acid wet etching further enhances surface smoothness by eliminating roughness, resulting in optical-quality surfaces suitable for high-efficiency diffraction applications. Figure 5(c) shows the surface of the grating and corresponds to a roughness RMS of 0.2 nm.

We characterized the precision capabilities of our e-beam methodology through goniometer based laser measurements at HZB[19] of our VLS grating patterns fabricated across the entire large curved substrates. The comparison between measured and designed pitch values across 120 mm optical area on a 140 mm long substrate shows excellent agreement with the sub-nanometer accuracy and remarkable precision (see Fig. 6).

The polynomial density relationship $a_0 + a_1x + a_2x^2 + a_3x^3$ was successfully implemented with high accuracy, achieving residuals of 0.001 lines/mm for the reciprocal base density (a_0 = 800 lines/mm), 0.002 mm^{-1} for the first-order coefficient, 5×10^{-6} mm^{-2} for the second-order term, and 2×10^{-7} mm^{-3} for the third-order coefficient, likely hitting the limit of the laser technique (details about the technique can be found in Ref. 20). These results validate the

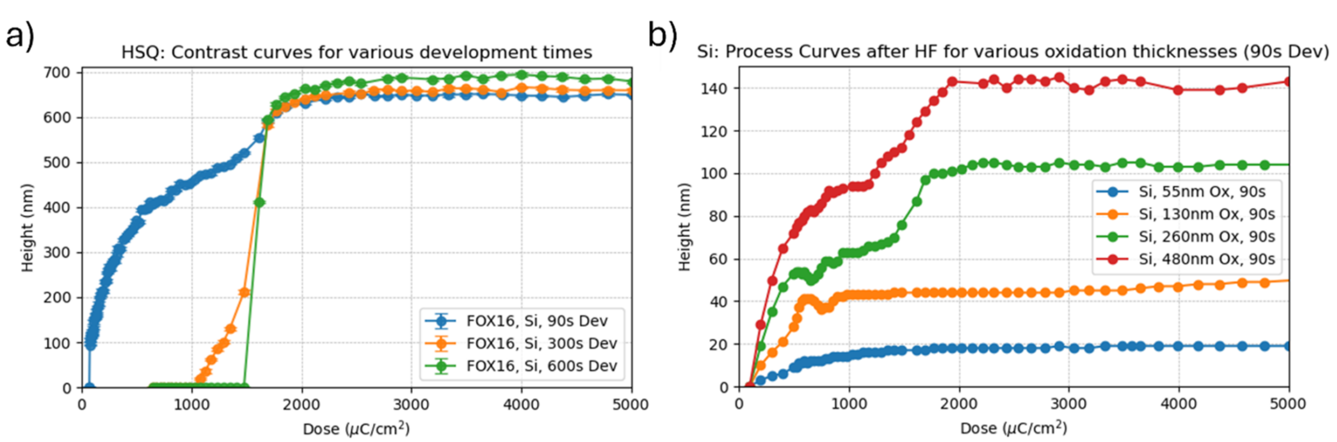

FIG. 4. Dose response behavior—development time and oxidation thickness curves. (a) Contrast curves of HSQ resist on silicon substrates for different development times (90, 300, and 600 s). The measured resist height as a function of electron beam dose demonstrates the impact of development duration on the dose response and achievable grayscale modulation. (b) Silicon height after SiO_2 removal (mask profile as a comparison to the final Si surface profile), after various through-mask oxidation thicknesses, resulting in transferred grayscale heights in Si as a function of exposure dose.

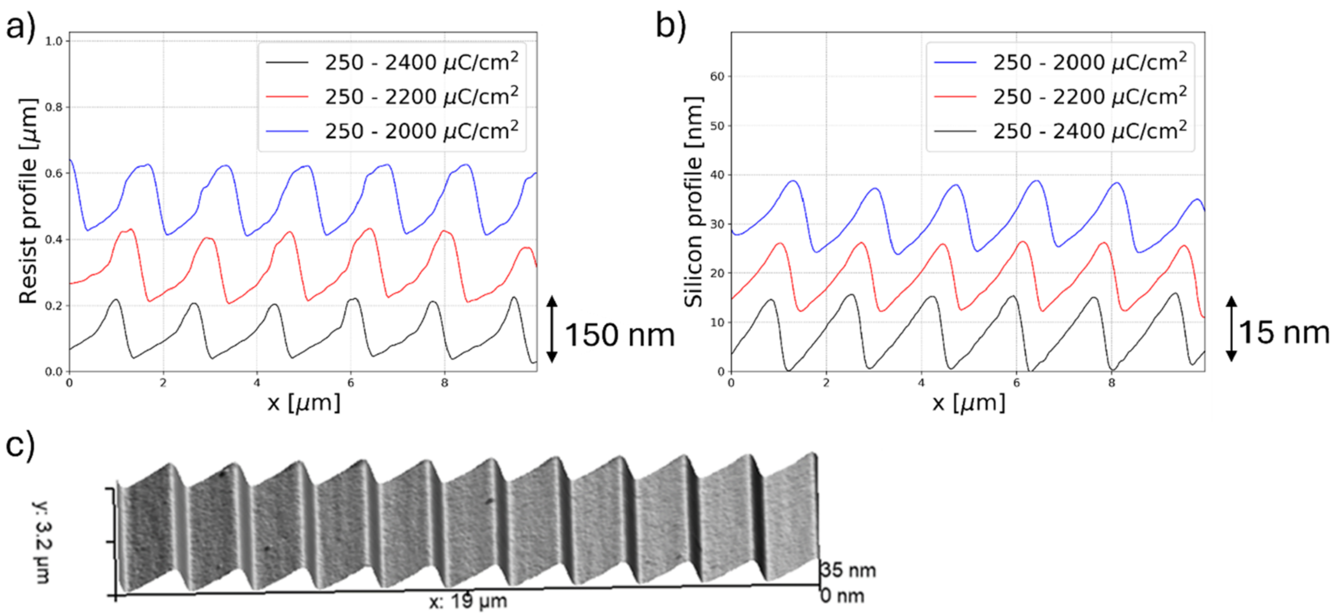

FIG. 5. (a) AFM traces of the HSQ resist on Si displaying 150 nm height variations. (b) AFM traces of the Si grating after 1100 °C thermal oxidation following the HF etch removal of oxide, illustrating significant smoothing of the original profile and a tenfold reduction down to 15 nm. (c) Final silicon surface achieving sub-nanometer roughness (RMS = 0.2 nm) suitable for high-efficiency diffraction.

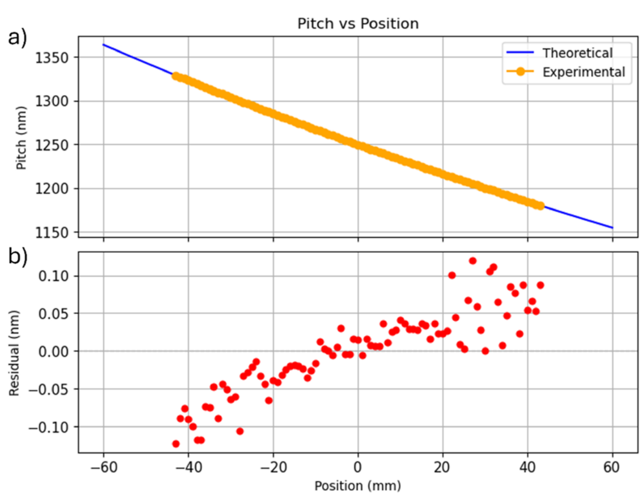

FIG. 6. Large-area pitch uniformity assessment for VLS grating across a substrate. Laser goniometry measurement results with (a) measured (yellow) vs designed (blue) pattern pitch as a function of stage position x, confirming a polynomial decrease from 1360 to 1150 nm over 120 mm. (b) Residual plot of pitch deviation from design, indicating maximum deviations within ±120 pm across the measured 80 mm.

effectiveness of continuous field scaling techniques in achieving third order polynomial densities at sufficient accuracy required for synchrotron applications.

The maximum residual in pattern pitch across the entire optical area of 120×20 mm^2 on a $140 \times 30 \times 10$ mm^3 substrate was measured using goniometry laser measurements[19] to be less than 120 pm, see Fig. 6 bottom graph. This precision level represents a significant advancement over conventional fabrication techniques and meets stringent requirements for next-generation x-ray optics applications.

Throughput and scalability advantages

The continuous field scaling approach enables higher line densities to be fabricated within the same exposure time as lower density gratings. However, fabricating higher densities will need to optimize the grayscale lithography to achieve the necessary smoothly varying grooves and high anti-blaze angles that require abrupt changes in height. This combination can be achieved by varying the development time of the HSQ. Unlike mechanical ruling, where a diamond tool with a maximum ruling velocity of 10 mm/sec writes line by line, thus increasing the writing time with increasing line density; the EBL approach maintains a constant throughput regardless of the local grating period. This capability becomes particularly valuable for VLS gratings where line densities vary continuously across the substrate according to the polynomial relationships and other requirements of flexibility, such as freeform structures.

The writing speeds achieved represent conservative estimates based on the current system capabilities; modern throughput-oriented EBL instruments utilize significantly higher beam currents compared to the research-focused systems employed here. For instance, the latest tools achieve currents up to 350 nA, instead of the 150 nA employed here, offering a direct improvement in writing time by a factor of 2.3.

CONCLUSIONS

We demonstrate that advanced electron beam lithography strategies achieve sub-nanometer line pitch control for variable line spacing gratings on large, curved substrates, meeting stringent requirements of synchrotron and free-electron laser applications. The integration of continuous field scaling, multi-pass exposures, and novel dose mapping techniques enables the fabrication of complex VLS patterns with polynomial density variations while maintaining exceptional precision across the 120×20 mm^2 optical area of the $140 \times 30 \times 10$ mm^3 substrate.

Our breakthrough in non-linear dose mapping methodology reduces data preparation complexity by forty times, while preserving full compatibility with existing high-precision placement strategies. Combined with the through-mask oxidation pattern transfer, this approach delivers high optical-quality blazed gratings with smooth surface finishes and sub-nanometer pitch control while being varied continuously. These results validate electron beam lithography as a viable alternative to limited mechanical ruling infrastructure, offering superior flexibility and precision for next-generation x-ray optics.[21,22]

Future developments will focus on leveraging higher throughput EBL systems with increased complexity in the designs, such as freeform x-ray optics, but also higher beam currents, step frequencies to further enhance writing speeds while maintaining the demonstrated precision and optical quality.

ACKNOWLEDGMENTS

This project has received funding from the European Union's Horizon 2020 research and innovation program under Grant Agreement No. 101004728.

AUTHOR DECLARATIONS

Conflict of Interest

V.A.G. and C.D. have a patent (U.S. Patent 12,287,498) related to the fabrication method described in this manuscript.

Author Contributions

K.H. and N.S. contributed equally to this work with sample preparation, data curation, analysis, and methodology. B.A.F. assisted in the preparation of the data, samples, and measurements. K.J. assisted with sample preparation. A.F.H., T.S., and F.S. performed the laser goniometry measurements. B.K. and C.Z. lead the implementation of the dose shape gradients. V.A.G. assisted with sample preparation, AFM measurements, and methodology. C.D. supported in sample fabrication, data analysis, and funding acquisition. K.H. prepared the original draft, and all co-authors contributed to the review and editing of this manuscript.

Kevin Hofhuis: Conceptualization (lead); Data curation (lead); Formal analysis (lead); Investigation (lead); Methodology (lead); Visualization (lead); Writing – original draft (lead); Writing – review & editing (equal). **Nazanin Samadi**: Conceptualization (lead); Data curation (lead); Formal analysis (lead); Investigation (lead); Methodology (lead); Visualization (equal); Writing – review & editing (equal). **Bjarke A. Frederiksen**: Data curation (equal); Investigation (supporting); Methodology (supporting); Visualization (supporting); Writing – review & editing (supporting). **Konstantins Jefimovs**: Investigation (supporting); Methodology (supporting); Writing – review & editing (supporting). **Analía F. Herrero**: Data curation (equal); Investigation (supporting); Validation (supporting); Writing – review & editing (supporting). **Tino Seliger**: Data curation (supporting); Methodology (supporting); Writing – review & editing (supporting). **Frank Siewert**: Investigation (supporting); Validation (supporting); Writing – review & editing (supporting). **Bas Ketelaars**: Methodology (supporting); Project administration (supporting); Software (lead); Writing – review & editing (supporting). **Christiaan Zonnevylle**: Funding acquisition (supporting); Methodology (supporting); Project administration (supporting); Software (lead); Writing – review & editing (supporting). **Vitaliy A. Guzenko**: Conceptualization (lead); Data curation (equal); Investigation (equal); Methodology (equal); Software (lead); Supervision (lead); Validation (equal); Writing – review & editing (supporting). **Christian David**: Data curation (supporting); Funding acquisition (lead); Methodology (supporting); Supervision (lead); Writing – review & editing (supporting).

DATA AVAILABILITY

The data that support the findings of this study are available within the article and its figures.

REFERENCES

[1] R. Reininger, "The in-focus variable line spacing plane grating monochromator," Nucl. Instrum. Methods Phys. Res., Sect. A **649**, 139–143 (2011).

[2] L. J. P. Ament, M. van Veenendaal, T. P. Devereaux, J. P. Hill, and J. van den Brink, "Resonant inelastic x-ray scattering studies of elementary excitations," Rev. Mod. Phys. **83**, 705–767 (2011).

[3] Q. Li, W. Chen, S. Liu, and L. Tong, "Structural topology optimization considering connectivity constraint," Struct. Multidiscip. Optim. **54**(4), 971–984 (2016).

[4] K.-J. Zhou, A. Walters, M. Garcia-Fernandez, T. Rice, M. Hand, A. Nag, J. Li, S. Agrestini, P. Garland, H. Wang, S. Alcock, I. Nistea, B. Nutter, N. Rubies, G. Knap, M. Gaughran, F. Yuan, P. Chang, J. Emmins, and G. Howell, "I21: An advanced high-resolution resonant inelastic x-ray scattering beamline at diamond light source," J. Synchrotron Radiat. **29**, 563–580 (2022).

[5] R. H. Hessel, R. L. Schmoys, and W. F. Shy, "Gratings for maximum efficiency," J. Opt. Soc. Am. **65**, 380–384 (1975).

[6] L. Braicovich, L. J. P. Ament, V. Bisogni, F. Forte, C. Aruta, G. Balestrino, N. B. Brookes, G. M. De Luca, P. G. Medaglia, F. M. Granozio, M. Radovic, M. Salluzzo *et al.*, "Magnetic excitations and phase separation in the cuprates from resonant inelastic x-ray scattering," Phys. Rev. Lett. **102**, 167401 (2009).

[7] J. Amann, W. Berg, V. Gorkhover, W. T. Elser, A. R. Khan, N. Tiedtke, S. Bajt, P. Emma, V. Shah, L. B. Wiegart, S. Zhu, E. R. Woods, and R. Grübel, "Demonstration of self-seeding in a hard-x-ray free-electron laser," Nat. Photonics **6**, 693–698 (2012).

[8] F. Senf, F. Bijkerk, F. Eggenstein, G. Gwalt, Q. Huang, R. Kruijs, O. Kutz, S. Lemke, E. Louis, M. Mertin, I. Packe, I. Rudolph, F. Schäfers, F. Siewert, A. Sokolov, J. M. Sturm, C. Waberski, Z. Wang, J. Wolf, T. Zeschke, and A. Erko, "Highly efficient blazed grating with multilayer coating for tender x-ray energies," Opt. Express **24**, 13220–13230 (2016).

[9] J. Gaudin, S. Rajagopal, S. Toleikis, J. Krzywinski, H. Sinn, N. Stojanovic, and H. Zacharias, "Investigating the interaction of x-ray free-electron laser radiation with grating structure," Opt. Lett. **37**(15), 3247–3249 (2012).

[10] J. Krzywinski, M. Kuhlmann, D. Khakhulin, K. Sokolowski-Tinten, and T. Tschentscher, "Damage thresholds for blaze diffraction gratings and grazing incidence optics at an x-ray free-electron laser," J. Synchrotron Radiat. **25**, 19–25 (2018).
[11] F. Siewert, U. Teubner, K. Batkov, V. Guzenko, T. Tiedtke, J. Goss, D. Zerfass, H. Gorke, F. Scholze, H. Soltau, F. Scholze, and A. Siewert, "Gratings for synchrotron and FEL beamlines: A project for the manufacture of ultra-precise gratings at helmholtz zentrum Berlin," J. Synchrotron Radiat. **25**, 91–99 (2018).
[12] R. Steingrüber and Z. Zhang, "High performance gratings for DFB lasers fabricated by direct-write e-beam lithography," SPIE Proc. **10032**, 100320C (2016).
[13] A. B. Liu, R. Cao, J. Y. Lu, and Y. Y. Yin, "New varied-line-spacing diffraction gratings for high-resolution monochromators," J. Opt. Soc. Am. A **23**, 1135–1140 (2006).
[14] F. Siewert, J. Buchheim, T. Zeschke, H. Lammert, V. Guzenko, and F. Senf, *The Nanometer Optical Component Measuring Machine: A New sub-nm Topography Measuring Device for X-ray Optics at BESSY* (AIP Publishing, 2004).
[15] J. C. Wyant, "White Light Interferometry," Proc. SPIE **4737**, 98–107 (2002).
[16] C. David and V. A. Guzenko, "Fabrication of blazed diffractive optics by through-mask oxidation," U.S. Patent 12,287,498 (Apr 2025).
[17] U. Kleineberg, K. Osterried, H.-J. Stock, D. Menke, B. Schmiedeskamp, D. Fuchs, P. Müller, F. Scholze, K. F. Heidemann, B. Nelles, and U. Heinzmann, "Mo/Si multilayer-coated ruled blazed gratings for the soft-x-ray region," Appl. Opt. **34**, 6506–6512 (1995).
[18] M. Lubov and L. Goray, "High-efficiency x-ray multilayer-coated blazed gratings with shifted boundaries," J. Synchrotron Radiat. **26**, 1539–1545 (2019).
[19] Verein Deutscher Ingenieure, VDI/VDE-Richtlinie 5575 Blatt 10: Schichtdickenmessung mit optischen Methoden–Blatt 10: Weißlicht-Interferometrie, Düsseldorf, Germany, 2002).
[20] S. Lemke, S. Alimov, J. Knedel, O. Kutz, I. Rudolph, T. Seliger, and A. Sokolov, *Low Line Density Blazed Gratings with Low Blaze Angles* (IOP Publishing, Zurich, Switzerland, 2022).
[21] A. Sokolov, Q. Huang, F. Senf, J. Feng, S. Lemke, S. Alimov, J. Knedel, T. Zeschke, O. Kutz, T. Seliger, F. Schäfers, F. Schäfers, F. Siewert, I. V. Kozhevnikov, R. Qi, Z. Zhang, W. Li, and Z. Wang, "Optimized highly efficient multilayer-coated blazed gratings for the tender x-ray region," Opt. Express **27**, 16833–16846 (2019).
[22] Q. Huang, I. V. Kozhevnikov, A. Sokolov, Y. Zhuang, T. Li, J. Feng, F. Siewert, J. Viefhaus, Z. Zhang, and Z. Wang, "Theoretical analysis and optimization of highly efficient multilayer-coated blazed gratings with high fix-focus constant for the tender x-ray region," Opt. Express **28**, 821–845 (2020).